RSC Advances

PAPER

View Article Online
View Journal | View Issue

Cite this: *RSC Adv.*, 2014, **4**, 26081

Synthesis of polymeric lubricating films directly at the sliding interface *via* mechanochemical reactions of allyl alcohols adsorbed from the vapor phase

Anthony J. Barthel, Daniel R. Combs and Seong. H. Kim*

Received 15th March 2014
Accepted 30th May 2014

DOI: 10.1039/c4ra02283a

www.rsc.org/advances

Ensuring lubrication effects during disruption of lubricant molecule supply is an important objective for boundary lubrication. Friction tests conducted in an allyl alcohol vapor environment yielded a friction coefficient near 0.25, which was significantly lower than the values (>0.6) measured for unlubricated contacts, and produced a tribopolymer where contact occurred. No tribopolymer was created outside the contact area, and the underlying substrate was not worn inside the contact area. A tribopolymer film created during 800 cycles of allyl alcohol vapor flow could lubricate sliding contacts for 30 000 cycles even after allyl alcohol vapor supplied was ceased. No significant wear or friction increase was observed during these cycles. Infrared spectroscopy analysis of the slide contact area indicated that the tribopolymer is a polyalcohol formed by polymerization of the allylic group. No tribopolymer formation was observed for vapor phase lubrication with saturated normal alcohols. The tribopolymer created from allyl alcohol vapor must be mechanochemically synthesized within the sliding interface. Such a mechanochemical synthesis of polymeric lubricant film could be applied to boundary lubrication of micro-scale devices.

Introduction

Conformal application and reliability are two essential lubricant properties for micro- and nano-scale devices with sliding parts. Approaches to lubricate and protect micro-electromechanical systems (MEMS) surfaces have often relied on organic monolayers or hard coatings;[1–3] but these methods have issues with wear over a device lifetime.[4] Silicon is an important substrate material for small scale devices due to its well-established lithography techniques, but the silicon surface is highly susceptible to wear in dry conditions and even more in humid conditions.[5–7] Conformal lubrication of silicon surfaces has been accomplished using vapor phase lubrication (VPL) to supply adsorbed alcohol molecules to the sliding surfaces. It was found that a monolayer of adsorbed *n*-pentanol in equilibrium with the vapor phase can reduce friction and eliminate wear of a silicon surface.[8] The wear of silicon in a humid environment may involve hydrolysis reactions when the counter surface is SiO_2 but not with a diamond counter surface, indicating that both mechanical pressure and surface chemistry of the counter surface play important roles.[9]

VPL by *n*-pentanol only lubricates adequately when a monolayer of adsorbed molecules is present at the silicon surface through continuous replenishment and the contact pressure does not exceed the critical material properties. The absence of *n*-pentanol vapor coincides with the loss of lubrication and the onset of surface wear. Wear due to insufficient adsorbed molecules or exceeding the mechanical properties of the silicon substrate led to the formation of polymeric species within the wear track. Polymer production was negligible on non-worn Si surfaces indicating that Si dangling bonds exposed upon surface wear catalyze the polymer formation.[10]

Other materials show similar trends. Adsorbed water vapor can cause severe adhesive wear or galvanic corrosion between sliding metal contacts.[11,12] *n*-Pentanol VPL is able to greatly reduce friction and wear for self-mated stainless steel as well as many other materials that exhibit high friction and wear in a dry inert or humid environment.[13] This friction and wear reduction does not result in any tribopolymer creation on these inorganic solid surfaces and lubrication ceases when vapor supply ends. The mechanochemical formation of a tribopolymer is essential to protect sliding surfaces in the absence of continuous vapor supply.

Mechanochemistry is a field that deals with nonthermal chemical reactions that occur due to mechanical energy.[14–16] Mechanochemical reactions occur at all length scales but detailed information on their yield and selectivity are lacking, especially at the micro and nano-scale. This is further complicated by processes such as triboemission and the creation of

Department of Chemical Engineering and Materials Research Institute, Pennsylvania State University, University Park, PA 16802, USA. E-mail: shkim@engr.psu.edu

triboplasmas.[17] Molecules at the material surface during boundary lubrication are under high contact pressure and frictional shear and thus the energy needed for mechanochemical reactions to occur is already present. Not all adsorbed molecules undergo mechanochemical reactions or give triboproducts that are beneficial to lubrication, so it is essential to understand how molecular structure impacts polymer formation and lubricity. Detrimental triboproducts were initially observed in telephone switching applications but has also been observed in MEMS devices.[18,19]

In this study, we investigate the lubrication and mechanochemistry attributes of allyl alcohol vapor. The unsaturated C=C double bond in the allylic alkyl is hypothesized to be polymerized *via* mechanochemical mechanisms without involvement of reactive dangling bonds of the solid exposed by surface wear. Vapor pressure and applied load are modified to elucidate tribopolymer formation characteristics and the addition of other vapors is studied to determine the robustness of the mechanochemically synthesized lubricant. Infrared spectroscopy is used to confirm the tribopolymer formation at the sliding track. The resiliency of the tribopolymer created during the vapor adsorption conditions is tested in a dry inert environment to investigate lubrication in the absence of lubricant supply. Findings on the nature of the tribopolymer created by allyl alcohol vapor are discussed within the scope of mechanochemistry and lubricant additive chemistry.

Experimental details

Friction tests were performed on a home-built tribometer with a reciprocating ball-on-flat geometry. All tests were conducted with AISI 440C stainless steel (SS) substrates that were polished with successively finer grit sandpaper and finally with 1 μm colloidal alumina solution. RMS roughness of the SS substrates was below 40 nm. A 3 mm diameter 440C SS ball with an RMS roughness below 10 nm (after removal of sphere curvature) was used as a counter-surface. Material surfaces were cleaned with ethanol followed by UV/ozone treatment to remove any contaminants. The applied load varied in some experiments but was kept at 0.2 N unless otherwise noted. The tribometer operated at a sliding velocity of 0.4 cm s^{-1} and created a wear track that was roughly 2.5 mm in length.

Vapor test environments were created by mixing a saturated vapor stream and a dry inert stream in the desired ratios. The saturated vapor stream was created by flowing an inert gas through a liquid column filled with the test liquid. Saturation vapor pressure (p_{sat}) of allyl alcohol and other liquids at room temperature and all partial pressures of the vapors are expressed as a percent relative to saturation ($p/p_{sat} \times 100\%$). The p_{sat} of allyl alcohol is 23 Torr at room temperature.

The lubrication efficiency of tribopolymers was also studied. First, allyl alcohol vapor was supplied during the first 800 cycles of the friction test and then the vapor flow was stopped. Friction tests continued in dry nitrogen to investigate the lubricating effect of the polymer created during the vapor-lubricated cycles.

Optical profilometry analysis was conducted *ex situ* to measure the wear track dimensions using a Zygo NewView 7300 in ambient conditions. An optical microscope was used to visually inspect the wear track. Polarization-modulation reflection absorption infrared spectroscopy (PM-RAIRS) spectra used to analyze vapor and adsorbate species were collected using a Thermo-Nicolet Nexus 670 spectrometer with an MCT-a detector. The IR spectra of tribopolymer piles around the slide track were obtained using a Hyperion 3000 Microscope coupled to IFS 66/s spectrometer with an MCT-a detector.

Results and discussion

Friction tests were conducted in various conditions to understand the nature of tribopolymer formation of allyl alcohol on stainless steel. Fig. 1a displays the friction data for self-mated stainless steel tests at varying pressure of allyl alcohol compared to a dry nitrogen environment. Friction in dry nitrogen is high and unstable, with the friction coefficient fluctuating between 0.6 and 1.0 for the majority of cycles. This unlubricated sliding results in catastrophic wear of both the flat substrate and the spherical ball. Fig. 1b shows an optical microscope image as well as an optical profilometry image of the wear track produced on the flat substrate in a nitrogen atmosphere. The black regions in the microscope image indicate areas of high roughness in which light is scattered away from the microscope aperture. The deep grooves and high plateaus can extend several microns from the original unworn surface.[12]

The introduction of allyl alcohol vapor reduces friction substantially across a large range of vapor pressures tested in this study. All the partial pressure of saturation (p/p_{sat}) conditions tested exhibited similar friction behavior (Fig. 1a). Friction coefficient values for p/p_{sat} varying within 15–80% stayed between 0.2–0.26 for the majority of reciprocating cycles. There is no clear trend that distinguishes higher vapor pressure from lower vapor pressure, indicating that as long as there is at least 15% p/p_{sat} of allyl alcohol vapor present, lubrication of sliding stainless steel contacts will occur.

Fig. 1c and d shows optical microscope images of the wear track for selected allyl alcohol tests. The wear tracks are much narrower than the wear track produced in dry nitrogen, and there is no catastrophic wear. Instead, a triboproduct can be observed at the edges as well as ends of the wear track. The images show a thin film-like substance with variable thickness indicated by an iridescent color that accumulates at the edges and ends of the wear track. This triboproduct film was not removed when rinsed or sonicated with ethanol or acetone for several minutes. Physically rubbing the film with a cotton swab wet with solvents removed the film. The wear track beneath the film exhibited no clear wear marks other than plastic deformation of surface asperities (Fig. 1e).

Fig. 2a shows the effect of varying load on friction for a 30% p/p_{sat} allyl alcohol environment. Similarly to Fig. 1a, the friction coefficient for the different loads shown in Fig. 2a stays between 0.2–0.26 for the majority of reciprocating cycles and there is no clear increasing or decreasing trend of friction coefficient with varying applied load. The optical microscope images in Fig. 2b–e show the end of the wear track where a large amount of triboproduct is found. This product is visibly similar for all

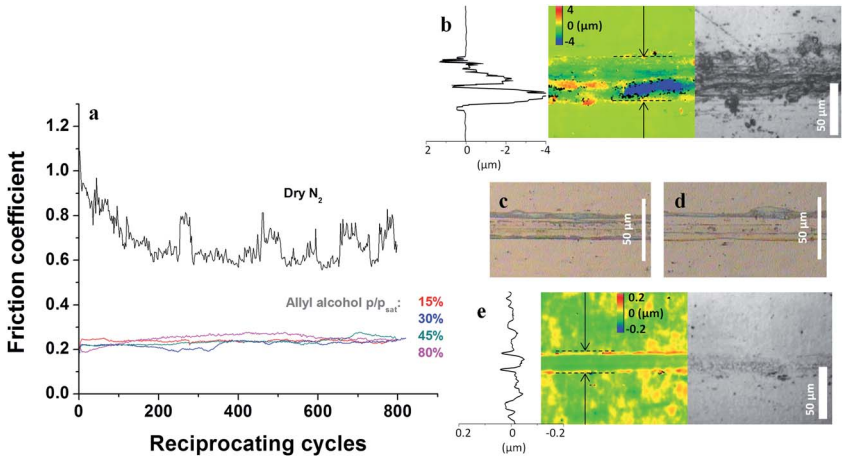

Fig. 1 (a) Friction coefficient for stainless steel *versus* stainless steel in different dry and allyl alcohol vapor environments. (b) Optical microscope (right), optical profilometry (center) and line profile (left) traced across the wear track for a dry nitrogen environment. The line profile is traced across the optical profilometry image following the black arrows and the dotted lines represent the edge of the wear track. (c and d) Optical microscope image of the wear track and triboproduct created at 15% p/p_{sat} (c) and 45% p/p_{sat} (d). (e) Optical microscope (right), optical profilometry (center) and line profile (left) traced across the wear track for an allyl alcohol environment. The triboproduct has been washed away so that surface wear can be seen.

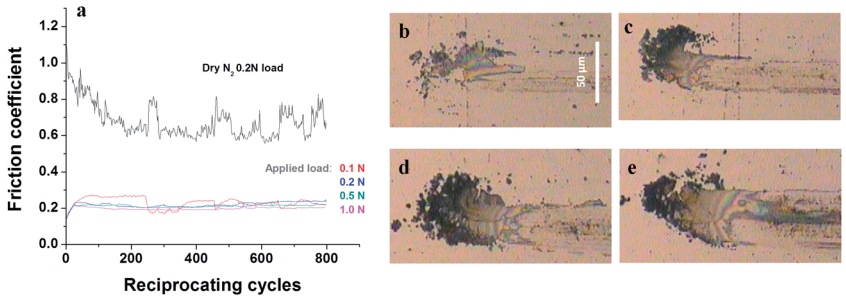

Fig. 2 (a) Friction coefficient for stainless steel *versus* stainless steel for different applied loads in a 30% p/p_{sat} allyl alcohol vapor environment. (b–e) Optical microscope images of the wear track ends and triboproduct created under 0.1 N (b), 0.2 N (c), 0.5 N (d), and 1.0 N (e). The scale bar in (b) applies to all images.

applied loads and seems to increase in quantity as applied load increases. Colorful regions indicate thin film interference due to changing thickness of the triboproduct film, and black areas indicate a thick build-up of the film material. Determining the quantitative dependence of triboproduct formation on applied pressure is difficult due to the widening of the wear tracks and inability to measure the triboproduct volume using optical profilometry. Hertzian mechanics dictates that a 0.1 N load will result in an approximately 20 μm wide wear track and 370 MPa contact pressure for self-mated stainless steel. This increases to nearly 40 μm and 800 MPa for a 1.0 N load. The wider contact area allows for greater formation of triboproduct during sliding and thus greater accumulation near the wear track edges and ends. This will occur in addition to any pressure-induced triboproduct formation changes.

Comparing the visible images in Fig. 1 and 2 yields possible insights as to the importance of vapor pressure and mechanical pressure on the formation of allyl alcohol triboproduct. Varying vapor partial pressure within 15–80% p/p_{sat} seems to have negligible effect on the yield of triboproduct, indicating a zeroth order reaction with respect to vapor pressure. Triboproduct formation increases with frictional force (= applied load × friction coefficient) and at a seemingly greater rate than the contact area increase with the load. The zeroth order reaction with respect to vapor pressure could indicate that roughly a monolayer coverage of allyl alcohol adsorbate was maintained at the tested vapor conditions, keeping the reactant concentration constant. If the allyl alcohol adsorption isotherm is similar to normal alcohol adsorption isotherms, the average adsorbate thickness for a p/p_{sat} range of 15–80% is expected to be close to the monolayer coverage.[20] The positive dependence on the friction force indicates that greater force allows for more mechanochemical reactions. As the force on a chemical bond increases, the potential energy of the chemical bond may decrease, lowering the activation energy for reaction.[21]

Triboproduct formation by allyl alcohol seems to be influenced by the presence of other vapors, but the lubrication effect by the vapor adsorption is not diminished substantially. Fig. 3a shows the friction coefficient values for allyl alcohol with water vapor and allyl alcohol with *n*-pentanol vapor. Friction

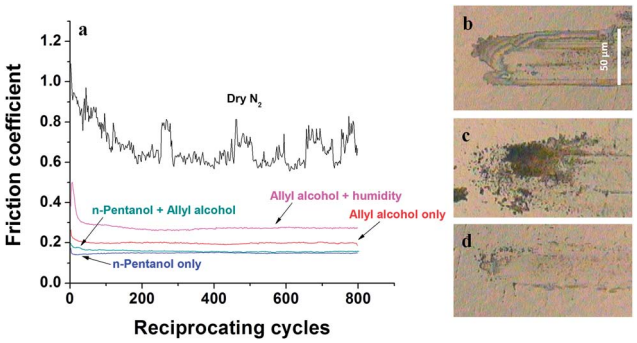

Fig. 3 (a) Friction coefficient for stainless steel *versus* stainless steel for different vapor environments. (b–d) Optical microscope images for wear track ends and triboproduct created under (b) an allyl alcohol environment, (c) an allyl alcohol and water vapor environment, (d) an allyl alcohol and *n*-pentanol environment. The scale bar in (b) applies to all images.

coefficient values for an environment of allyl alcohol with water vapor initially begin high, with a value near 0.5 during the first few cycles. This value steadily decreases and reaches a steady value of ~0.3 after 50 cycles. This steady value is slightly higher than that the typical values seen in an environment of only allyl alcohol vapor. The initially high friction in the presence of water vapor occurred for multiple tests across multiple samples, indicating that it is not due to specimen differences but due to competitive co-adsorption of vapors. Once sufficient amount of triboproduct is formed in the first ~50 cycles, the water co-adsorption effect on friction seems diminished although it has profound effects on triboproduct yield and deposition pattern. Fig. 3b and c shows optical images of the wear track for allyl alcohol with and without water vapor. Both wear tracks show significant triboproduct formation although there is a distinct difference in the aggregation pattern of the triboproduct. The film produced in vapor containing allyl alcohol only is more continuous and shows the iridescent thin film interference whereas the film produced from mixed vapors of allyl alcohol and water appears much more particulate and discrete. Although the film characteristics appear different in these two cases, both give similar friction coefficients.

Fig. 3a also shows friction behavior for *n*-pentanol vapor as well as *n*-pentanol vapor plus allyl alcohol vapor. The dual flow case exhibits similar friction behavior to *n*-pentanol vapor (both with friction near 0.15) and each case is lower than the case with allyl alcohol vapor only. *n*-Pentanol vapor has previously been shown to lubricate surfaces well with minimal wear and a friction coefficient near 0.15.[13] Optical images of the wear track indicate that triboproduct formation is nearly absent for the dual flow case and the only *n*-pentanol vapor case.

The friction data from these mixed vapor flow cases suggests that friction is dominated by the more lubricious molecule although competitive adsorption of both components is likely.[22] Allyl alcohol plus water vapor eventually gives friction similar to pure allyl alcohol vapor, but the initial friction cycles are high and the tribopolymer produced looks markedly different from pure allyl alcohol. Partial coverage of the surface by adsorbed water could explain these differences. Likewise, *n*-pentanol and allyl alcohol vapor give minimal triboproduct and a friction coefficient similar to pure *n*-pentanol. These results implied that the surface is dominated by adsorbed *n*-pentanol with small amounts of adsorbed allyl alcohol during the friction test.

Infrared spectroscopy was conducted on the triboproduct to characterize the chemical species present. Fig. 4 shows the spectrum for allyl alcohol vapor as well as the spectrum of allyl alcohol layer adsorbed on copper and the triboproducts produced on the rubbed surface. The spectra primarily focus on the alkyl and hydroxyl stretching vibration regions. The vapor spectrum shows two distinct regions: a sharp peak near 3650 cm^{-1} indicative of free OH stretching vibration and a group of peaks around 3000 cm^{-1} that come from alkyl vibrations. The peak at 3100 cm^{-1} comes from the asymmetric CH_2 stretching vibration of unsaturated carbons associated with the allyl group.[23] The remaining peaks from 3000–2850 cm^{-1} arise from allylic CH_2 symmetric stretch and alkyl stretching vibrations. A comparison between the vapor and adsorbate spectra yields one clear difference in the OH stretching region. The sharp free-OH peak at 3650 cm^{-1} is absent and a broad, weak peak centered near 3400 cm^{-1} appears. The broad peak implies hydrogen bonding interactions of allyl alcohol molecules in the adsorbed layer.[24] The peaks due to the alkyl chains do not change position appreciably and intensity changes are difficult to distinguish due to low signal to noise in the adsorbate spectrum.

The two spectra of triboproducts shown in Fig. 4 were obtained from environments of allyl alcohol and allyl alcohol plus water vapor as well. These spectra share many similarities between themselves, and there is one clear distinction between the triboproduct spectra and the adsorbed molecule spectrum. The characteristic allyl peak at 3100 cm^{-1} that is seen in both the vapor and adsorbed allyl alcohol spectra is not present in either of the triboproduct spectra. Although thin film interference effects add undulations to the product spectra that are especially visible between 3000 and 4000 cm^{-1}, the triboproduct appears to have a broad peak near 3400 cm^{-1} that is similar to the adsorbed allyl alcohol spectrum. The triboproduct retains the alkyl stretching peaks between 3000 and 2800 cm^{-1}.

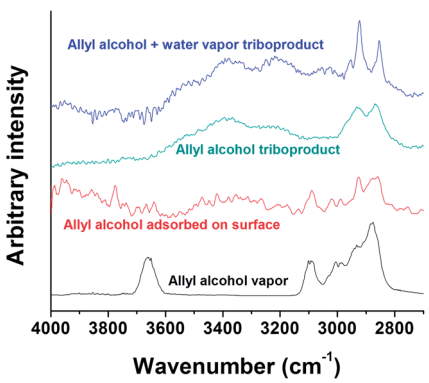

Fig. 4 Infrared spectra for allyl alcohol vapor (black), allyl alcohol adsorbed on copper (red), and the triboproducts created in an allyl alcohol vapor environment (cyan) and an allyl alcohol and water vapor environment (blue).

These spectral features indicate that the adsorbed allyl alcohol reacts under pressure or sliding to create a polyalcohol film that does not desorb into the vapor phase. Polymerization of allyl alcohol by pulsed radio frequency plasma shows a similar tendency, where the allyl vibration that is initially present becomes absent upon polymerization.[25] The polymer infrared spectrum still retains the broad OH stretching peak near 3400 cm^{-1} as well as the alkyl stretching peaks near 3000 cm^{-1}.

Friction tests of this polymer in the absence of continuous vapor supply were conducted to assess the lubricity of the tribopolymer. Fig. 5 shows friction tests in which the tribosystem operated in an allyl alcohol vapor environment for the first 800 cycles, after which vapor flow ceased and a dry inert gas was introduced for the remainder of the test. The only lubricant that would be present for these remaining cycles is what was produced from the vapor during the initial cycles. The friction for the initial cycles run in allyl alcohol vapor was near the typical value of 0.25. When the sliding cycle was resumed in the dry inert gas environment, the friction coefficient was a bit higher (0.4–0.5) initially and then quickly decreased to a steady friction coefficient of ~0.25. The initial high friction upon the resumption of the sliding after removal of the allyl alcohol supply was observed for almost all test trials. From the optical images shown in Fig. 1 and 2, the triboproducts are mostly piled outside the wear track. During the 800 cycles of sliding in allyl alcohol vapor, the slide track is mostly covered with allyl alcohol adsorbates keeping a low surface energy and triboproducts are squeezed out to the periphery. When the allyl alcohol vapor is removed, the adsorbates are now desorbed and the surface energy of the slide track region will increase. Then the polymeric triboproduct (polyalcohols) can flow in and wet the wear track. The reciprocating motion of the counter-surface could help the transport of the triboproduct from the periphery to the sliding region and at the same time it can keep the triboproduct layer thickness in the slide track to a certain minimal value.

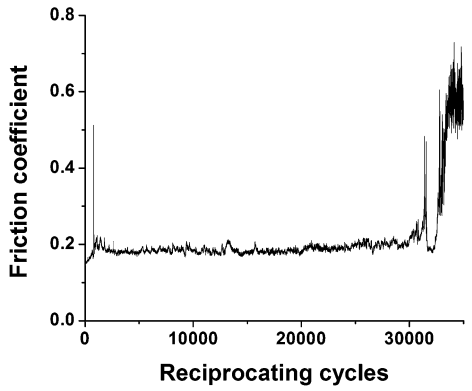

Fig. 5 Friction coefficient for stainless steel *versus* stainless steel to test the lubricity of the synthesized triboproduct in the absence of supplied allyl alcohol vapor. The first 800 cycles were conducted in an allyl alcohol vapor environment, after which the vapor flow ceased and only dry nitrogen was supplied. The friction spike above 0.5 at the left side of the graph corresponds to the cessation of vapor flow.

After the cessation of the allyl alcohol vapor supply, lubrication was maintained for over 32 000 cycles by the polyalcohols that were produced in 800 cycles, demonstrating its efficacy to continuously lubricate the sliding interface in the absence of vapor supply. Eventually, lubrication failed after ~32 000 cycles with friction increasing above 0.5 and severe adhesive wear occurring at the rubbing interface. At this moment, all triboproduct produced initially during the 800 'synthesis' cycle must be consumed or squeezed out of the wear track.

The tribopolymer formation that transforms allyl alcohol into a polyalcohol must occur through mechanisms substantially different than typical pressure-induced polymerization processes. The contact pressures experienced during sliding is in the range of 0.3–0.5 GPa. Asperities undergoing deformation may see higher pressure, but tribopolymer is formed throughout the duration of the friction test and most asperities are flattened during the initial cycles. Polymerization through pressurizing gases requires an order of magnitude higher pressure and occurs at much slower rates, typically many hours or even days. Molecules such as carbon monoxide and cyanogens undergo polymerization at pressures above 5 GPa and 10 GPa, respectively.[26,27] Acrylic acid polymerization initiates at ~8 GPa while the polymerization of ethylene occurs above 3.6 GPa and takes several hundred hours.[28,29] The contact pressures and sliding speed in the tribology tests are low enough that flash temperature increases due to frictional heating is only a few Kelvin.[30] Unlike vinyl monomers, allyl compounds have very low activity in thermally-activated free-radical polymerization reactions due to allylic chain transfer process.[31]

The origins of tribopolymer formation in allyl alcohol and *n*-pentanol are completely different. *n*-Pentanol vapor is able to form tribopolymers on silicon surfaces only when surface wear occurs, exposing highly-reactive dangling Si bonds at the wear track.[6] The *n*-pentanol tribopolymer is absent when there is no surface wear. Thus, the *n*-pentanol polymerization is *via* tribochemical reactions at the surface defects formed during the wear process. The friction tests conducted with allyl alcohol do not show surface wear when the polymer is removed from the stainless steel (Fig. 1b), meaning that allyl alcohol polymerizes by a mechanochemical mechanism under interfacial pressure and shear actions that does not involve the reactive surface atoms. More details of the mechanochemical reaction mechanism could not be established at this time. Better understanding of reaction mechanism requires more thorough chemical analyses for elemental composition and molecular weight distribution of the tribopolymers.

The mechanochemical synthesis of polymeric lubricant films from the adsorbed allyl alcohol molecules provides several advantages for conformal friction and wear reduction. Tribopolymer synthesis due to repeated sliding or application of pressure means that synthesis only occurs where it is needed. Vapor adsorbs on all surfaces but tribopolymer will not contaminate areas where there are no frictional interactions. Additionally, the lubrication of both the adsorbed alcohol and the subsequent polymer allow for continued lubrication during the absence of vapor supply. The polymer is synthesized as

needed during vapor flow but causes no ill effects to continued lubrication.

The mechanochemical reactivity of allyl alcohol, especially compared to saturated normal alcohols, yields insights into the role of unsaturated hydrocarbons used as additives in liquid lubricants. Determining the mechanochemical reactivity of liquids can be challenging due to the underlying physics of liquid lubrication. Applied load may be spread over a larger area or thicker lubricant film, prohibiting the pressures necessary for tribopolymerization. If a tribopolymer is formed, it may dissolve back into the bulk liquid which has chemically similar structure or functional groups or be physically removed due to viscous forces. Analyzing a triboproduct formed from a liquid is complicated by residual liquid that may be entrapped in the wear track. The data presented here clearly show that the unsaturated hydrocarbons can be polymerized due to the applied load and shear at the sliding contact.

On-site synthesis of lubricating polymers can be utilized in areas where consistent application of lubricant cannot be guaranteed. This is especially important in applications where intermittent and unintended contact occurs during operation or where surfaces slide infrequently, such as during start-up and shut down processes.[32,33] The formation of a persistent lubricant only at contacting surfaces allows for a potent lubrication strategy without detrimental polymer formation in non-contacting regions.

Conclusions

The effects of adsorbed allyl alcohol vapor and the subsequently formed tribopolymer film on the friction and wear of stainless steel were investigated. Allyl alcohol vapor yields a friction coefficient near 0.25 and negligible wear of sliding surfaces. The unsaturated C=C bond in allyl alcohol polymerizes under interfacial pressure and shear to give a polyalcohol that can lubricate surfaces in the absence of continuous supply of lubricating vapor. The tribopolymer is mechanochemically synthesized only where sliding occurs, thus delivering lubricant onto the surfaces where it is required.

Acknowledgements

This work was supported by the National Science Foundation (Grant no. CMMI-1000021).

Notes and references

1 R. Maboudian, W. R. Ashurst and C. Carraro, *Sens. Actuators, A*, 2000, **82**, 219–223.
2 S. A. Smallwood, K. C. Eapen, S. T. Patton and J. S. Zabinski, *Wear*, 2006, **260**, 1179–1189.
3 S. Onclin, B. J. Ravoo and D. N. Reinhoudt, *Angew. Chem., Int. Ed.*, 2005, **44**, 6282–6304.
4 S. H. Kim, D. B. Asay and M. T. Dugger, *Nano Today*, 2007, **2**, 22–29.
5 D. B. Asay, M. T. Dugger and S. H. Kim, *Tribol. Lett.*, 2008, **29**, 67–74.
6 A. L. Barnette, D. B. Asay, D. Kim, B. D. Guyer, H. Lim, M. J. Janik and S. H. Kim, *Langmuir*, 2009, **25**, 13052–13061.
7 A. Opitz, S.-U. Ahmed, J. Schaefer and M. Scherge, *Wear*, 2003, **254**, 924–929.
8 D. B. Asay, M. T. Dugger, J. A. Ohlhausen and S. H. Kim, *Langmuir*, 2008, **24**, 155–159.
9 D. J. Marchand, L. Chen, Y. Meng, L. Qian and S. H. Kim, *Tribol. Lett.*, 2014, **53**, 365–372.
10 A. L. Barnette, D. B. Asay, J. A. Ohlhausen, M. T. Dugger and S. H. Kim, *Langmuir*, 2010, **26**, 16299–16304.
11 J. Lancaster, *Tribol. Int.*, 1990, **23**, 371–389.
12 A. J. Barthel, M. D. Gregory and S. H. Kim, *Tribol. Lett.*, 2012, **48**, 305–313.
13 A. J. Barthel and S. H. Kim, *Langmuir*, 2014, DOI: 10.1021/la501049z, in press.
14 M. K. Beyer and H. Clausen-Schaumann, *Chem. Rev.*, 2005, **105**, 2921–2948.
15 S. L. James, C. J. Adams, C. Bolm, D. Braga, P. Collier, T. Friscic, F. Grepioni, K. D. M. Harris, G. Hyett, W. Jones, A. Krebs, J. Mack, L. Maini, A. G. Orpen, I. P. Parkin, W. C. Shearouse, J. W. Steed and D. C. Waddell, *Chem. Soc. Rev.*, 2012, **41**, 413–447.
16 G. Kaupp, *CrystEngComm*, 2009, **11**, 388–403.
17 K. Nakayama and J.-M. Martin, *Wear*, 2006, **261**, 235–240.
18 H. Hermance and T. Egan, *Bell Syst. Tech. J.*, 1958, **37**, 739–776.
19 L. Chen, H. Lee, Z. Guo, N. E. McGruer, K. Gilbert, S. Mall, K. D. Leedy and G. G. Adams, *J. Appl. Phys.*, 2007, **102**, 074910–074917.
20 A. L. Barnette, D. B. Asay, M. J. Janik and S. H. Kim, *J. Phys. Chem. C*, 2009, **113**, 10632–10641.
21 M. K. Beyer, *J. Chem. Phys.*, 2000, **112**, 7307–7312.
22 A. L. Barnette and S. H. Kim, *J. Phys. Chem. C*, 2012, **116**, 9909–9916.
23 R. A. Nyquist, *Interpreting infrared, Raman, and nuclear magnetic resonance spectra*, Academic Press, 2001.
24 A. L. Barnette, D. B. Asay, M. J. Janik and S. H. Kim, *J. Phys. Chem. C*, 2009, **113**, 10632–10641.
25 C. L. Rinsch, X. Chen, V. Panchalingam, R. C. Eberhart, J.-H. Wang and R. B. Timmons, *Langmuir*, 1996, **12**, 2995–3002.
26 W. Evans, M. Lipp, C.-S. Yoo, H. Cynn, J. Herberg, R. Maxwell and M. Nicol, *Chem. Mater.*, 2006, **18**, 2520–2531.
27 C. S. Yoo and M. Nicol, *J. Phys. Chem.*, 1986, **90**, 6732–6736.
28 C. Murli and Y. Song, *J. Phys. Chem. B*, 2010, **114**, 9744–9750.
29 D. Chelazzi, M. Ceppatelli, M. Santoro, R. Bini and V. Schettino, *J. Phys. Chem. B*, 2005, **109**, 21658–21663.
30 J. Archard and R. Rowntree, *Wear*, 1988, **128**, 1–17.
31 A. Fahmy, A. Schönhals and J. r. Friedrich, *J. Phys. Chem. B*, 2013, **117**, 10603–10611.
32 D. P. Hess and A. Soom, *J. Tribol.*, 1990, **112**, 147–152.
33 S. V. Canchi and D. B. Bogy, *IEEE Trans. Magn.*, 2010, **46**, 764–769.

